

1 Response to reviewer #1

2 Comments from reviewer #1 are in black while our response in red and changes in the manuscript
3 are in blue.

4 **1. General comments** This manuscript presents original data on NO photoproduction from nitrite
5 in seawater samples from the northwestern Pacific Ocean. The two cruise tracks add substantially
6 to the rather scant data coverage in open ocean waters so far. NO photochemistry is linked to the
7 production of reactive species such as the hydroxyl radical and is therefore of wider interest for
8 ocean scientists. The manuscript is therefore relevant to the scope of Ocean Science. The methods
9 used for the photochemical irradiations and sample analyses largely seem sound although their
10 description requires some additional detail (see specific comments below).

11 Thank you very much for your advice. The manuscript was amended, and you will find a detailed
12 description in how we took all the comments and suggestions into account in the preparation of the
13 revised manuscript.

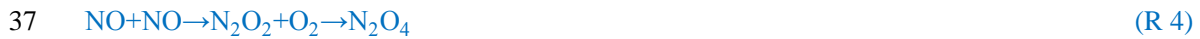
14 Aspects of the authors' interpretation of the irradiation results suffer from a rather narrow
15 perspective which neglects that nitrite and nitric oxide dynamics are tightly linked to a host of
16 reactive nitrogen and oxygen species in seawater. Authors should consider the available literature
17 in this regard in more detail, see for example Mack and Bolton (1999) who reviewed nitrate and
18 nitrate photolysis pathways and their interconnections. Given the complexity of the reaction
19 schemes in Mack and Bolton (1999) the absence of straightforward relationships between nitrite
20 and NO production is not surprising. The authors discussions of variability in NO photoproduction
21 rates could also be enhanced by considering factors other than nitrite concentration and light
22 intensity (e.g. NO_3^- , ocean optics, organic reactants, see e.g. De Laurentiis et al. (2015)).

23 Reports about nitrite and nitric oxide dynamics have been added to the Introduction and the Results
24 and Discussion parts (not showed here, showed in later part). The possible factors like NO_3^- , ocean
25 optics, organic reactants in natural seawater (like CDOM) and other influences in artificial seawater
26 were considered, and relevant references were also added like Mack and Bolton (1999); Kieber et
27 al. (1999); Minero et al. (2007), and so on.

28 “Apart from (micro)biological processes, NO can be produced photochemically from dissolved
29 nitrite (NO₂⁻) in the sunlit surface ocean (Zafiriou and True, 1979; Zafiriou and McFarland, 1981):



31 Mack and Bolton (1999) had reviewed the possible subsequent reaction, for example: the produced
32 NO and OH could react to produce HNO₂ reversely (R2), and some reactions that consumed NO
33 like R4 to R7



40 In natural sunlit seawater, photolyzed dissolved nitrate (NO₃⁻) could also be a potential source of
41 NO through NO₂⁻ (R 8)



43 In addition to NO₃⁻, dissolved organic matter sometimes could be a potential source of NO₂⁻ (Kieber
44 et al., 1999;Minero et al., 2007).”

45 I am also concerned about some aspects of wider interpretation in section 3.6. Estimates of NO sea-
46 to-air flux were based on steady state concentrations calculated from laboratory-derived
47 photoproduction rates and a poorly constrained scavenging rate with not discussion of the
48 uncertainties involved. As far as I can see, laboratory rates were not adjusted to ambient conditions,
49 although daily averaged irradiances in the tropical North Pacific are likely very different from those
50 in the solar simulator. Applying laboratory conditions here significantly overestimated relevant
51 photoproduction rates and therefore resulted in artificially enhanced NO steady state concentrations
52 and sea-to-air fluxes. This section will require thorough revision before publication.

53 We agreed that laboratory results overestimated relevant photoproduction rates. Thank you so much
54 for the advice on the ERA-5 data, the laboratory-derived photoproduction rates were adjusted into

55 the ambient photoproduction rates, based on the following added assumption: the rate of nitrite
56 photoproduction into NO was proportional to the irradiance flux in order to adjust the rates under
57 simulator light into ambient light at the sampling time (Zafiriou and McFarland, 1981). After the
58 adjustment, the rates became lower, which was understandable.

59 “Since the measured NO concentrations were not available from the cruise we estimated [NO] by
60 assuming that (1) NO production is mainly resulting from NO_2^- photodegradation, (2) the NO
61 photoproduction R_{NO} as measured in our irradiation experiment is balanced by the NO scavenging rate
62 R_s , (3) the rate of nitrite photoproduction into NO was proportional to the irradiance flux in order to
63 adjust the rates under simulator light into ambient light at the sampling time (Zafiriou and McFarland,
64 1981; Olasehinde et al., 2010):

$$65 \quad R_{\text{NO}} \times \frac{I_{\text{ambient}}}{I_{\text{simulator}}} = [\text{NO}] \times R_s, \quad (\text{EQ 1})$$

66 where R_s represents the sum of the rate constants for the scavenging compounds reacting with NO times
67 the concentrations of the scavenger compounds.”

68 Furthermore, the manuscript neglects to justify the validity of their approach to estimate NO steady
69 state concentrations from ‘surface rates’ (aka those measured in the laboratory) rather than from
70 depth integrated production rates for the upper mixed layer. This approach might be fine if the
71 timescales of mixing significantly exceed the timescales of photoproduction and scavenging.
72 However, this discussion is missing here.

73 On the one hand, the scavenging rates in our study were adopted from previous literatures (Zafiriou
74 and McFarland, 1981), and most scavenging rates were measured in the surface water samples.
75 Actually, the scavenging rates would change with the depth in the upper mixed layer. On the other
76 hand, the NO_2^- photolysis was the mainly source of NO because some reactions like nitrification in
77 the surface water was inhibited by light in the surface water. Thus, the NO concentration was
78 estimated from the photolysis of surface samplers. Furthermore, according to our study results in
79 the Yellow Sea and Bohai Sea, the photoproduction rates of NO were far higher than that of sea-to-
80 air exchange rates in the surface water (unpublished data), which suggested that many NO radicals
81 were scavenged and there were no significant difference between the surface NO concentration and
82 bottom NO concentration. Therefore, it seems reasonable to assume that the photoproduction rates

83 and the scavenging rates were faster than the mixing rates.

84 We add the following text to justify the validity of their approach.

85 “Tian et al (2018) found that NO concentration in the surface water showed no significant difference
86 with that in the bottom water (average depth: 43 m), so it seems reasonable to estimate the steady
87 state NO concentration with the NO concentration in the mixed layer.”

88 Furthermore, in the absence of photoproduction during night time hours sea surface NO levels will
89 be determined by the interplay between turbulent mixing and scavenging, and mixing is bound to
90 lower NO levels at the sea surface. This should also be considered by the authors. Further specific
91 comments are detailed below.

92 According to the study of Zafiriou and McFarland (1981) and relevant studies, NO in the surface
93 seawater seemed under detection limit after sunset, thus when adjusting into the ambient light
94 intensity, the rates and NO concentration were estimated to 0.

95 2. Specific and editorial comments

96 **Abstract:** The abstract is rather vague, does not give any quantitative information, does not spell
97 out how many irradiations were carried out and what oceanic regions were covered. Please add the
98 relevant detail.

99 The abstract has been rewritten with quantitative data results from the present study.

100 “Nitric oxide (NO) is a short-lived intermediate of the oceanic nitrogen cycle. However, our
101 knowledge about its production and consumption pathways in oceanic environments is rudimentary.
102 In order to decipher the major factors affecting NO photochemical production, we irradiated
103 artificial seawater samples as well as 31 natural surface seawater samples in laboratory experiments.
104 The seawater samples were collected during a cruise to the western tropical North Pacific Ocean
105 (WTNP, a N/S section from 36 to 2 °N along 146/143 °E with 6 and 12 stations, respectively, and a
106 W/E section from 137 to 161 °E along the equator with 13 stations) from November 2015 to January
107 2016. NO photoproduction rates from dissolved nitrite in artificial seawater showed increasing
108 trends with decreasing pH, increasing temperatures and increasing salinity. In contrast, NO
109 photoproduction in the natural seawater samples from the WTNP did not show any correlations with

110 pH, water temperature and salinity as well as dissolved nitrite concentrations. NO photoproduction
111 rates (average: $0.5 \pm 0.2 \times 10^{-12} \text{ mol L}^{-1} \text{ s}^{-1}$) in the WTNP were significantly larger than the NO air–
112 sea flux densities (average: $1.8 \times 10^{-12} \text{ mol m}^{-2} \text{ s}^{-1}$) indicating a further NO loss process in the surface
113 layer.”

114 **Introduction** The introduction is exceedingly brief and gives hardly any context regarding
115 inorganic nitrogen photochemistry in aquatic systems. Again, authors should refer to Mack and
116 Bolton (1999), and refer to key pathways involved. For example, it would be well worth mentioning
117 that nitrate photolysis to nitrite and nitrite photolysis to NO occur in parallel and that there are
118 various NO consumption pathways.

119 The background about inorganic nitrogen photochemistry in aquatic systems has been included in
120 the introduction part. The key pathways of NO scavenging and the following reactions were added:

121 “Apart from (micro)biological processes, NO can be produced photochemically from dissolved
122 nitrite (NO_2^-) in the sunlit surface ocean (Zafiriou and True, 1979; Zafiriou and McFarland, 1981):



124 Mack and Bolton (1999) had reviewed the possible subsequent reaction like the produced NO and
125 OH could react to produce HNO_2 reversely (R2), and some reaction that consumed NO like R4 to
126 R7



133 In natural sunlit seawater, photolyzed dissolved nitrate (NO_3^-) could also be a potential source of
134 NO through NO_2^- (R 8) (Carpenter and Nightingale, 2015; Benedict et al., 2017)



136 In addition to NO_3^- , dissolved organic matter sometimes could be a potential source of NO_2^- (Kieber
137 et al., 1999; Minero et al., 2007).”

138 **lines 33 ff:** This sentence merely lists previous papers on NO photoproduction without any
139 discussion of available results. To provide adequate context, the authors should add relevant
140 quantitative information on the variability of NO production rates and discuss suggested reasons for
141 this variability.

142 The sentence has been amended to include some quantitative information about NO production rates,
143 the relevant NO concentration and NO lifetime, and previous papers were discussed.

144 “Table 1 summarized studies about photochemical production of NO measured in the surface waters
145 of the equatorial Pacific Ocean (Zafiriou et al., 1980; Zafiriou and McFarland, 1981), the Seto Inland
146 Sea (Anifowose and Sakugawa, 2017; Olasehinde et al., 2009; 2010), the Bohai and Yellow Seas
147 (Liu et al., 2017, Tian et al., 2018) and the Kurose River (Japan) (Olasehinde et al., 2009; Anifowose
148 et al., 2015). NO photoproduction rates varied among different seawater samples, it seems the rates
149 in Kurose River (average: $499 \times 10^{-12} \text{ mol L}^{-1} \text{ s}^{-1}$) was biggest, which was possibly due to an
150 increase of nitrite being released into the river in agricultural activity during the study time. However,
151 NO concentration was about $1.6 \times 10^{-12} \text{ mol L}^{-1}$, at lowest level, which was because of higher
152 scavenging speed in river water (lifetime :0.25 s). The lifetime of NO showed increasing trend from
153 river (several seconds) to inland sea (dozens of seconds) to open sea (dozens to hundreds of seconds),
154 reviewed in Anifowose and Sakugawa (2017). NO also showed higher concentration level in coastal
155 waters than open sea, higher photoproduction rates might account for this.”

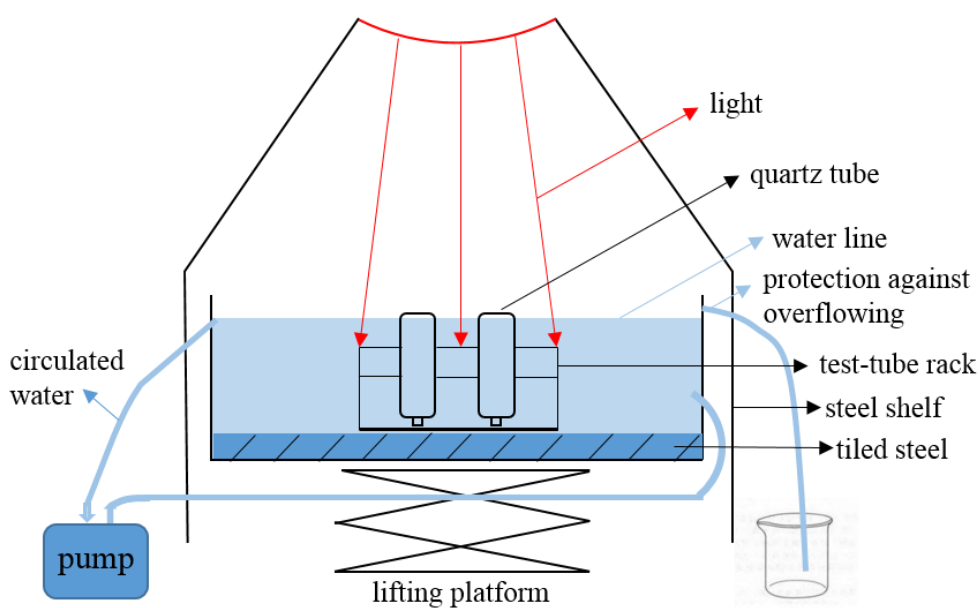
156 **Methods Lines 57 ff, Detection limits:** Please explain how you calculated these – are they based
157 on triplicate analyses?

158 Further detail has been added about the detection limit. The detection limit and relative standard
159 error were based on 7 times. The detection limit concentration was determined by $S/N=3$ (3×0.03)
160 with 7 blank samples (only DAF-2 in artificial seawater) and the slope (0.101) in the low
161 concentration range ($3.3 - 33 \times 10^{-10} \text{ mol L}^{-1}$).

162 “The detection limit concentration was determined by $S/N=3$ (3×0.03) with the blank samples (7)
163 and the slope (0.101) in the low concentration range ($3.3 - 33 \times 10^{-10} \text{ mol L}^{-1}$).”

164 **Lines 65 ff, Temperature control:** It is unclear how samples were irradiated, and how temperature
165 was controlled. Please describe irradiation flasks/ cuvettes used (material, dimensions, optical
166 pathlength) and explain if they were immersed in a water bath or if they were water jacketed to
167 allow for water cooling. If samples were immersed did you correct for the effects of immersion on
168 irradiance?

169 The irradiation experiment has been amended as suggested. Fig. R1 is a simple profile figure of the
170 SUNTEST CPS+ solar simulator (ATLAS, Germany) with a thermostatic pump ((LAUDA Dr. R.
171 Wobser GmbH & Co. KG, Germany) in a water bath. The SUNTEST CPS+ was lifted on a steel
172 shelf, and there was a box with a lifting platform. Bottom of the box, there was another tiled steel
173 with a lot of square hole, and the test-tube rack was tied to the tiled steel. The hole on the second
174 floor of the test-tube rack was filled with silica gel flower pat which could prevent the cuvettes
175 floated (Fig. R2). The height of the cylindrical quartz cuvette was 70 mm and inner diameter was 14
176 mm with the volume about 10 mL (optical pathlength was the height about 70 mm). During the
177 experiment, the 10 mL sample in the quartz cuvette was blocked by PTFE stopper, and the mouth
178 of the quartz cuvette was wrapped by parafilm to avoid leak and being polluted. In our experiments,
179 the samples were installed in the SUNTEST CPS+ solar simulator and a little higher than the water
180 bath surface.



181

182 Figure R1. Simple profile figure of the SUNTEST CPS+ solar simulator with the thermostatic

183

pump.



184

185

Figure R2. The test-tube rack.

186 “The temperature of the photochemical reaction was 20 °C, controlled by a thermostatic pump
187 ((LAUDA Dr. R. Wobser GmbH & Co. KG, Germany). The height of cylindroid quartz cuvette used
188 for irradiation was 70 mm and the inner diameter was 14 mm with the volume about 10 mL. The
189 optical pathlength was about 70 mm. During the experiment, the quartz cuvette, filled with 10 mL
190 sample and blocked by PTFE stopper, was a little higher than the water bath surface.”

191 **Line 74:** How were subsamples collected?

192 When sampling, the SUNTEST CPS+ was turned off and triplicate subsamples were collected from
193 each sample in dark with microsyringe (50 µL), and then the cuvettes were quickly put back into
194 the water bath to continue the experiment until two hours.

195 “Triplicate samples from each treatment were collected every 0.5 h with an entire irradiation time
196 of 2 h. At the sampling time, the SUNTEST CPS+ was turned off and triplicate subsamples were
197 collected from each sample in dark with microsyringe (50 µL), and then the cuvettes were quickly
198 put back into the water bath to continue the experiment until two hours.”

199 **Lines 80, irradiance:** I understand that the Suntest CPS+ solar simulator provides 765 W m⁻² as
200 per manufacturer specifications. Measured lamp output is then given in units of Lux, which is a
201 photometric unit only. Please convert 60000 lx to units of W m⁻² for the spectral output of your
202 system. How did the actual solar simulator output compare to ambient sea surface irradiances during
203 the cruise?

204 In our system, the light irradiated on the sample was maintained at light intensity about 765 W m⁻²
205 (measured by internal radio meter), which is spectral output of our system. The illuminance was

206 measured about 60000 lx using (illuminance meter TP201704017, Zhejiang Top Cloud–Agri
207 Technology Co., Ltd, China). To avoid ambiguity, we would delete this description. The ERA-5
208 hourly data of our study cruise ranged from 0 (night)–873 W m⁻², with an average of 259 W m⁻²,
209 which was lower than the simulator. Thus, the laboratory-derived photoproduction rates were
210 adjusted into the ambient photoproduction rates as described above.

211 **Lines 103 ff, broadband filters:** please spell out the cut-off wavelengths of the 2 filter materials
212 used and add appropriate references.

213 In the study by Li et al. (2010), the films were described as: (1) full ambient sunlight (not wrapped),
214 (3) UV-A+Vis (wrapped with UV-B block film), (3) Vis (wrapped with UV block film). In the study
215 by Wu et al. (2015), the film were described as: Mylar film, which was purchased from United
216 States Plastic Cor. (Lima, Ohio), could only shield UVB. The other film, obtained from CPFilm Inc.,
217 USA, was a kind of car insulation film, which could shield both UVA and UVB. According to the
218 specification, the CPF film could shelter 99.7% UV (280–400nm) while Mylar film could shelter
219 UVB (280–320nm).

220 In order to compare the contributions of ultraviolet A (UVA), ultraviolet B (UVB) and visible light
221 to the NO photoproduction, two kinds of film light filters were used (wrapped around the quartz
222 glass tubes): (i) a Mylar plastic film (from United States Plastic Cor., Lima, Ohio) which can only
223 shield UVB (275–320nm) and (ii) a film, always used as car insulation film (from CPFilm Inc.,
224 USA) shielding both UVA and UVB (280–400nm) (Li et al., 2010;Wu et al., 2015).

225 The following references were added.

226 Li, Y., Mao, Y., Liu, G., Tachiev, G., Roelant, D., Feng, X., and Cai, Y.: Degradation of
227 methylmercury and its effects on mercury distribution and cycling in the Florida Everglades,
228 Environ. Sci. Technol., 44, 6661-6666, 2010.

229 **Lines 122 ff, seawater sampling:** please describe here how water samples were obtained.

230 The seawater sampling description was added to the section, as indicated below:

231 “A 750 mL black glass bottle was rinsed with in situ seawater three times, and then was filled with
232 seawater quickly through a siphon directly from the Niskin bottles. When the overflowed sample
233 reached the half volume of the bottle, the siphon was withdrawn rapidly, and the bottle was sealed

234 quickly.”

235 **Lines 139 ff, sample storage:** please give the maximum storage time from sample collection to
236 subsequent laboratory analysis.

237 It was about two months from the first sampling time to the laboratory analysis. Samples were stored
238 in darkness at 4 °C.

239 “the maximum storage time was about two months.”

240 **Results and Discussion Lines 169 ff, comparison with Anifowose et al. (2015):** your statement
241 “*The difference might be explained by different experimental set-ups such the different light sources*
242 *used in the irradiation experiments*” is too vague. Please give details on irradiance levels, and other
243 possible differences such as sample self-shading.

244 The irradiance in Anifowose et al. (2015) was about 2/3 as powerful as natural sunlight (at noon
245 under clear sky conditions in Higashi-Hiroshima city (34° 25' N) on May 1, 1998), but they don't
246 give exact value of irradiance level. The lamp power in our system was higher (1500 W), however,
247 the set-up should also be considered. In Anifowose et al. (2015), the quartz photochemical reaction
248 cell was 3 cm in diameter, 1.5 cm in length, and had a 6.5 mL capacity while in our study, the quartz
249 cuvette was 70 mm height and inner diameter was 14 mm with the volume about 10 mL, thus it
250 seemed that there are more sample self-shading effect in our study.

251 “The difference might be explained by different experimental set-ups such as sample self-shading,
252 in our study, the quartz cuvette was 70 mm height and inner diameter was 14 mm with the volume
253 about 10 mL while in Anifowose et al. (2015), the quartz photochemical reaction cell was 3 cm in
254 diameter, 1.5 cm in length, and had a 6.5 mL capacity.”

255 **Lines 172 ff, pH dependence:** while data on the pH dependence of NO photoproduction from nitrite
256 may be scant, there is substantial information available on hydroxyl radical production which – as
257 the authors state – is linked to NO: $\text{NO}_2^- + \text{H}_2\text{O} \rightarrow \text{NO} + \bullet\text{OH} + \text{OH}^-$ (equation 1) Again please refer
258 to the review in Mack and Bolton (1999) and to other more recent relevant literature, and give
259 further detail on previous findings.

260 It is agreed that the reactions of N_2O_4 and N_2O_3 hydrolysis reaction should be considered as reported

261 in Mack and Bolton (1999), and some new literatures were cited.

262 Carpenter, L. J., and Nightingale, P. D.: Chemistry and Release of Gases from the Surface Ocean,
263 Chem. Rev., 115, 4015-4034, 2015.

264 Benedict, K. B., Mcfall, A. S., and Anastasio, C.: Quantum Yield of Nitrite from the Photolysis of
265 Aqueous Nitrate above 300 nm, Environ. Sci. Technol., 51, 4387-4395, 2017.

266 “Tugaoen et al. (2018) also found the effect of lowering pH to conjugate NO_2^- to HONO allowed
267 for HONO photolysis (pH = 2.5). Besides, higher pH could also inhibit N_2O_4 and N_2O_3 hydrolysis
268 reaction (R4 and R7) as reported by Mack and Bolton (1999). However in previous studies of Chu
269 and Anastasio (2007) and Zellner et al. (1990), the quantum yield of OH (which equals to the
270 quantum yield of NO) was constant at the pH ranges from 6.0 to 8.0 and 5.0 to 9.0 under the
271 condition of single wavelength light in nitrite solution. This might indicate that decreasing pH in
272 our study mainly reduced NO consumption rather than increased NO production.”

273 **Lines 179 ff, temperature dependence:** Again, the description of results and their discussion are
274 too brief and lack detail. It would be interesting to see Arrhenius parameters, a note on the fact that
275 NO production at 0.5 μM nitrite did not increase from 20 to 30 $^\circ\text{C}$, and some plausible explanations
276 for that.

277 This section was amended to show results and their discussion. The Arrhenius formula parameters
278 were as following description. The plausible explanation of the rates from 20 to 30 $^\circ\text{C}$ was that NO_2^-
279 concentration here was the main influencing factor, NO_2^- might be run out at 20 $^\circ\text{C}$. If NO_2^-
280 concentration increased, like up to 5.0 $\mu\text{mol L}^{-1}$, the temperature could make a noticeable difference.

281 “Higher temperatures led to increasing NO photoproduction rates according to the temperature
282 dependence of chemical reactions given by the Arrhenius formula:

$$283 R = A \times \exp\left(-\frac{E}{R \times T}\right) \quad (\text{EQ 2})$$

284 where A is an Arrhenius prefactor and T is the temperature (K). This indicates that an increasing
285 temperature results in a higher rate, Chu and Anastasio (2007) also found that the quantum yield of OH
286 or NO showed a decreasing trend from 295K, 263K to 240K. Moreover, this equation can be used to
287 consider the difference of the rates at two temperatures T_1 and T_2 :

288 $R_{T2} = R_{T1} \times \exp\left(\frac{E}{R} \times \left(\frac{1}{T1} - \frac{1}{T2}\right)\right)$ (EQ 3)

289 If it was assumed that E was a constant in the temperature ranges of 10 to 30 °C when $\text{NO}_2^- = 0.5 \mu\text{mol}$
290 L^{-1} , and plotting $\ln R$ against $1/T$, the E value was obtained as $57.5 \text{ kJ mol}^{-1} \text{ K}^{-1}$. Using the
291 photoproduction rate at 20 °C (293.15 K) as our reference point (T1), an expression of the R_T with the
292 temperature was as follows:

293 $R_T = 2.7 \times 10^{-10} \times \exp\left(6920 \times \left(\frac{1}{293.15} - \frac{1}{T2}\right)\right)$ (EQ 4)

294 Similarly, we could conclude expression of the R_T with the temperature when $\text{NO}_2^- = 5.0 \mu\text{mol L}^{-1}$,

295 $R_T = 7 \times 10^{-10} \times \exp\left(11026 \times \left(\frac{1}{293.15} - \frac{1}{T2}\right)\right)$ (EQ 5)

296 However, the NO production rate at 0.5 μM nitrite did not increase from 20 to 30°C. The reason could
297 be attributed to that NO_2^- concentration here was the main influencing factor, NO_2^- might be run out at
298 20 °C. If NO_2^- concentration increased, like up to $5.0 \mu\text{mol L}^{-1}$, the temperature could make a noticeable
299 difference.”

300 **Lines 182 ff, salinity dependence: Again, this is too brief and lacks detail. At the very least**
301 **there should be some quantitative statement on the observed salinity dependence, if not some**
302 **parameterization.**

303 Salinity dependence has been discussed and the quantitative statement was added, as indicated
304 below.

305 “Higher salinity obviously enhanced photoproduction rates of NO in both Milli-Q water and
306 artificial seawater samples with the initial NO_2^- concentrations of 0.5 or $5.0 \mu\text{mol L}^{-1}$. The linear
307 regression relationship is $y = 0.37x - 4.55$ for $0.5 \mu\text{mol L}^{-1} \text{NO}_2^-$ and $y = 2.3x - 39.5$ for $5.0 \mu\text{mol}$
308 $\text{L}^{-1} \text{NO}_2^-$, respectively, where x is the salinity (‰) and y is the photoproduction rate ($\times 10^{-10} \text{ mol L}^{-1}$
309 s^{-1}). This result indicates that with the increasing ion strength NO production is enhanced, however,
310 the exact mechanism is unknown and need further study. Zafriou and McFarland (1980) also
311 demonstrated that artificial seawater comprised with major and minor salts showed complex
312 interactions. However, Chu and Anastasio (2007) reported that added Na_2SO_4 ($4.0\text{--}7.0 \text{ mmol L}^{-1}$)
313 in solution had no effect on the quantum yield of OH.”

314 **Lines 187 ff, broadband wavelength dependence:** Again, some additional detail would be useful.
315 What are the percentage contributions to the various wavelength ranges (UVB, UVA, Vis)? Another
316 minor niggle: The nitrite absorption maximum according to Zuo and Deng (1998) is at 354 nm, not
317 at 356 nm as stated in line 192. Please clarify.

318 The contribution of visible band, UVA band and UVB band were <1.0%, 30.7 % and 85.2 % for 0.5
319 $\mu\text{mol L}^{-1} \text{NO}_2^-$, respectively (sum>1 because of experimental error) and <1%, 34.2 % and 63.1 % for 5.0
320 $\mu\text{mol L}^{-1} \text{NO}_2^-$. The nitrite absorption maximum of 356 nm was corrected to 354 nm.

321 “The highest NO photoproduction rates were observed with full wave length band whereas the lowest
322 NO rates were observed with UVB. The NO photoproduction rates approached zero at wave lengths in
323 the visible. The contribution of visible band, UVA band and UVB band were <1%, 30.7 % and 85.2 %
324 (sum>1 because of experimental error) and <1%, 34.2 % and 63.1 % for 0.5 and 5.0 $\mu\text{mol L}^{-1} \text{NO}_2^-$,
325 respectively. Our results are in line with the findings of Zafiriou and McFarland (1981) who found that
326 samples exposed to (UV+visible) wave lengths lost NO_2^- more rapidly than those exposed only to visible
327 wave lengths alone. Chu and Anastasio (2007) found that under single wavelength light, quantum yield
328 of OH decreased with the wavelength (280 nm to 360 and plateau until 390) which meant that single
329 wavelength light of UVB had higher photoproduction rate than UVA. Since it might be because of the
330 wider band of UVA (320–420 nm) that lead to the total higher rates under UVA than UVB (in our system
331 300-320). Moreover, the photochemical NO_2^- degradation, as described in reaction (R 1), proceeds at
332 wave lengths of 300–410 nm with a λ_{max} of 354 nm, which is in the range of UVA (320–420 nm) (Zuo
333 and Deng, 1998; Zafiriou and McFarland, 1981).”

334 **Lines 195 ff, NO yield:** The statement that differences in yield may be due to “(unknown) nitrogen-
335 containing substrates” seems rather speculative. Can the authors explain what N-bearing
336 components could be present in pure laboratory water or artificial seawater? Another much more
337 plausible explanation would be that some nitrite reacts to N_2O_4 which then disproportionates to
338 nitrite and nitrate (Mack and Bolton, 1999).

339 The explanation was added to the revised manuscript as following statement. Besides, the
340 average % f_{NO} value in natural water samples was calculated based on the J_{NO} in artificial seawater.

341 “Another plausible explanation would be that during the photoproduction of NO_2^- , some NO were

342 oxidized into NO_2 , then NO_2 dimerized (R5) and the dipolymer N_2O_4 would hydrolyze into NO_2^-
343 and NO_3^- (R6), which actually reduce the concentration of NO_2^- (Mack and Bolton, 1999).”

344 “In our study, the average % f_{NO} value in natural water was 52%, indicating that there are other
345 unknown nitrogenous compounds, for example, NO_2^- produced from NO_3^- photolysis (R7) or other
346 organic matters which could further lead to NO production (Benedict et al., 2017;Goldstein and
347 Rabani, 2007;Kieber et al., 1999;Minero et al., 2007).”

348 **Line 210, DIN:** Please clarify if you tested for correlations with DIN only or also with its individual
349 components.

350 Individual components correlation with rates were analyzed.

351 “Photoproduction rates did not show significant correlations with NO_2^- , NO_3^- or NH_4^+ ”

352 **Line 211, CDOM:** What measure of colored dissolved organic matter did you use?

353 Absorbance spectra of CDOM in natural seawater samples were measured from 200 to 800 nm at 1
354 nm increment against a Milli-Q water reference using a UV-2550 UV-VIS spectrophotometer
355 (Shimadzu, Japan) with a quartz cell of 10 cm path length. A baseline correction was applied by
356 subtracting the absorbance value which was an average absorption from 700 nm to 800 nm from all
357 the spectral values mainly because of negligible CDOM absorption at this spectra range (Babin et
358 al., 2003). Absorption coefficient (α) were calculated as

359
$$\alpha = (2.303 \times A)/L,$$

360 where A is absorbance and L is the cell’s light path length in meters (Loh et al., 2004;Yang et al.,
361 2011), the absorption coefficient at 355 nm wavelength was assigned to CDOM concentration in
362 the present study (Blough et al., 1993;Zhu et al., 2017).

363 “Photoproduction rates did not show significant correlations with NO_2^- , NO_3^- , NH_4^+ , pH, salinity,
364 water temperature as well as colored dissolved organic matter (data not shown, the same method
365 with Zhu et al (2017))(statistics computed with SPSS v.16.0).”

366 **Lines 214 ff, correlations between NO production rates and nitrite:** Please give a quantitative
367 comparison between nitrite concentrations found in your and in previous work.

368 Relevant nitrite concentrations were added to Table 1 and minor modifications were made: Liu et
 369 al. (2017) and Anifowose and Sakugawa (2017) were added.

370 “In Table 1, the NO_2^- concentration of $0.06 \mu\text{mol L}^{-1}$ in our study was lower than most of other study
 371 area like Qingdao coastal waters ($0.75 \mu\text{mol L}^{-1}$) and the Seto Inland Sea ($0-0.4 \mu\text{mol L}^{-1}$ or $0.5-2 \mu\text{mol}$
 372 L^{-1}). In the study of Anifowose et al. (2015), since the NO_2^- concentration of upstream K1 station was
 373 similar to ours ($0.06 \mu\text{mol L}^{-1}$), the higher R_{NO} might attributed to lower pH (7.36) as mentioned above.”

374 **Table 1** Photoproduction rates (R), methods, average NO concentrations, NO_2^- concentrations and
 375 average flux densities of NO in different regions.

Regions	R ($\text{mol L}^{-1} \text{s}^{-1}$)	Methods	NO (mol L^{-1})	NO_2^- ($\mu\text{mol L}^{-1}$)	Flux ($\text{mol m}^{-2} \text{s}^{-1}$)	Sampling date	References
Seto Inland Sea, Japan	$8.7-38.8 \times 10^{-12}$	DAF-2	120×10^{-12}	0.5-2	3.55×10^{-12}	Oct 5–9, 2009	Olasehinde et al., 2010
Seto Inland Sea, Japan	$1.4-9.17 \times 10^{-12}$	DAF-2	$3-41 \times 10^{-12}$	$\sim 0.02-0.4$	0.22×10^{-12}	Sep, 2013 and Jun, 2014	Anifowose and Sakugawa, 2017
Kurose River, Japan	$9.4-300 \times 10^{-12}$	DAF-2	–	–	–	–	Olasehinde et al., 2009
Kurose River (K1 station), Japan	4×10^{-12}	DAF-2	1.6×10^{-12}	0.06	–	Monthly, 2013	Anifowose et al., 2015
Jiaozhou Bay	–	DAN	157×10^{-12}	–	7.2×10^{-12}	Jun, Jul and Aug, 2010	Tian et al., 2016
Jiaozhou Bay and its adjacent waters	–	DAN	$(160 \pm$ $130) \times 10^{-12}$	–	10.9×10^{-12}	Mar 8–9, 2011	Xue et al., 2011
Coastal water off Qingdao	1.52×10^{-12}	DAN	260×10^{-12}	0.75	–	Nov, 2009	Liu et al., 2017
Central equatorial Pacific	$> 10^{-12}$	Chemilum inescence	46×10^{-12}	0.2	2.2×10^{-12}	R/V Knorr 73/7	Zafiriou and Mcfarland., 1981
Northwest Pacific Ocean	$0.5 \pm 0.2 \times 10^{-12}$	DAF-2	49×10^{-12}	0.06	1.8×10^{-12}	Nov 15, 2015 to Jan 26, 2016	This study

376 Also, given that you compare your own open ocean data to results from coastal and estuarine waters,
 377 you should consider factors other than nitrite. For example, how could salinity changes or to changes
 378 in DOM levels and composition affect the relationship between nitrite and NO production?

379 **Salinity and other influencing factors were added.**

380 “In the study of Anifowose et al. (2015), since the NO_2^- concentration of upstream K1 station was similar
381 to ours ($0.06 \mu\text{mol L}^{-1}$), the higher R_{NO} might attributed to lower pH (7.36) as mentioned above. Or it
382 might be because of the discrepancy between the river water and the seawater, considering lower nitrite
383 level of K1, the higher R_{NO} might be attributed to dissolved organic matter. Because of its conservative
384 mixing behavior with salinity, dissolved organic matter always showed higher level in river than open
385 sea (Zhu et al., 2017), which could could photodegrade itself to produce NO_2^- , finally to promote R_{NO} .”

386 **Lines 220 ff, NO production rates:** Please refer to Table 1 at the start of this paragraph. Also, I
387 would expect some quantitative statements here, e.g. how much lower are your rates compared to
388 previous work. What other factors may have contributed to these differences (e.g. sea surface
389 irradiance, light attenuation?).

390 **Some quantitative statements were added here, for example, “the average photoproduction rate of NO**
391 **measured in our cruise ($0.5 \times 10^{-12} \text{ mol L}^{-1} \text{ s}^{-1}$)” and NO_2^- ($0.06 \mu\text{mol L}^{-1}$) in our study area.**

392 “Seen from Table 1, we can find that the average photoproduction rate of NO measured in our cruise (0.5
393 $\times 10^{-12} \text{ mol L}^{-1} \text{ s}^{-1}$) was lower than that of the Seto Inland Sea ($1.4\text{--}38.8 \times 10^{-12} \text{ mol L}^{-1} \text{ s}^{-1}$) and Kurose
394 River ($9.4\text{--}300 \times 10^{-12} \text{ mol L}^{-1} \text{ s}^{-1}$) which could be ascribed to higher background NO_2^- in the inland sea
395 and river waters (Olasehinde et al., 2009; 2010), in addition to our lower photoproduction rates during
396 nighttime. Our result is slightly lower than the R_{NO} from the central equatorial Pacific Ocean ($> 10^{-12}$
397 $\text{mol L}^{-1} \text{ s}^{-1}$), the lower concentration of NO_2^- ($0.06 \mu\text{mol L}^{-1}$) in our study area might account for this
398 (Zafiriou and McFarland, 1981). In the study of Anifowose et al. (2015), since the NO_2^- concentration
399 of upstream K1 station was similar to ours ($0.06 \mu\text{mol L}^{-1}$), the higher R_{NO} ($4 \times 10^{-12} \text{ mol L}^{-1} \text{ s}^{-1}$) might
400 attributed to lower pH (7.36) as mentioned reason above. Or it might be because the difference between
401 the river water and the seawater, considering lower nitrite level of K1, the higher R_{NO} might be attributed
402 to dissolved organic matter. Because of its conservative mixing behavior with salinity, dissolved organic
403 matter always showed higher level in river than in open sea (Zhu et al., 2017), which could photodegrade
404 itself to produce NO_2^- , finally to promote R_{NO} .”

405 **Lines 230 ff, air-sea flux densities:**

406 This section raises several issues. Firstly, you will need to give at least a brief statement summarizing

407 your approach even if details of calculations were provided elsewhere. This summary must contain
408 references to the air-sea gas exchange parameterization used and to the source of the Henry constant.

409 **Brief summarized statement about study approach and used references were included, as indicated**
410 **below.**

411 “The NO flux densities were computed with (EQ 6):

$$412 \quad F = k_{sea} ([NO] - pNO_{air} \times H^{cp}) \quad (EQ 6)$$

$$413 \quad pNO_{air} = x'NO_{air} \times (p_{ss} - p_w) \quad (EQ 7)$$

414 here F stands for the flux density (mass area⁻¹ time⁻¹) across the air-sea interface, k_{sea} is the gas
415 transfer velocity (length time⁻¹), c_{sea} is the measured concentration of NO in the surface seawater
416 (mass volumn⁻¹), $x'NO_{air}$ is the mixing ratio of atmosphere NO (dimensionless). The p_{ss} is the
417 barometric pressure while p_w was calculated after Weiss and Price (1980):

$$418 \quad \ln p_w = 24.4543 - 6745.09/(T + 273.15) - 4.8489 \times \ln (T + 273.15)/100 - 0.000544 \times S \quad (EQ 8)$$

419 H^{cp} is the Henry's law constant which is calculated after Sander (2015) as:

$$420 \quad H^{cp}(T) = H^\ominus \times \exp(-\Delta sol H/R \times (1/T - 1/T^\ominus)) \quad (EQ 9)$$

421 where $-\Delta sol \frac{H}{R} = \frac{d \ln H}{d \ln (\frac{1}{T})}$, H^\ominus , and $-\Delta sol H/R$ are tabulated ($-\Delta sol H/R=1600$ and $H^\ominus=1.9 \times 10^{-5}$ mol
422 m⁻³ pa⁻¹) in Sander (2015). Sander (2015) reviewed several literatures about NO H^\ominus and the values
423 in different literatures were similar. In our calculation, the value in the Warneck and Williams (2012)
424 were used.

425 Then k_{sea} was calculated after Wanninkhof (2014) as (EQ 10),

$$426 \quad k_{sea} = k_w (1 - \gamma_a) \quad (EQ 10)$$

427 γ_a is the fraction of the entire gas concentration gradient across the airside boundary layer as a
428 fraction of the entire gradient from the bulk water to the bulk air (dimensionless), k_a is the air side
429 air-sea gas transfer coefficient (length time⁻¹) of NO according to (Mcgillis et al., 2000; J ähne et al.,
430 1987; Sharqawy et al., 2010) for the details of the calculation of k_w and γ_a see Tian et al. (2018).”

431 Secondly, it is very unfortunate that no onboard wind speeds were available. Given that, the next
432 best solution would have been to use something like the ECMWF reanalysis data sets (e.g. ERA-5,

433 [https://cds.climate.copernicus.eu/cdsapp#!/dataset/reanalysis-era5-singlelevels?](https://cds.climate.copernicus.eu/cdsapp#!/dataset/reanalysis-era5-singlelevels?tab=overview) tab=overview)

434 which give hourly winds at 10 m above sea level.

435 Thank you very much for your advice. We have got the wind speed data (wind speed near the hourly

436 time was adopted, average: 5.55 m s^{-1}) and the irradiance data (light intensity at the sampling time

437 was estimated with interpolation method, average: 259 W m^{-2}).

438 Table R1: The wind speed and the light intensity from ECMWF reanalysis data sets (ERA-5)

Station	Wind speed (m s^{-1})	Light intensity (W m^{-2})
S0301	5.90	153.34
S0303	6.41	450.50
S0305	3.88	196.00
S0307	0.95	0.00
S0309	6.33	0.00
S0310	3.50	711.53
S0313	4.33	0.00
S0315	4.58	666.00
S0317	2.55	3.90
S0319	2.49	0.00
S0321	3.19	441.36
S0323	3.84	12.41
S0325	4.55	0.00
S0701	8.44	0.00
S0704	10.64	260.97
S0707	2.75	623.04
S0709	1.46	657.65
S0711	2.51	593.52
S0713	5.86	0.00
S0715	10.43	0.43
S0717	5.76	0.00
S0719	6.31	0.00
S0721	6.90	0.00
S0723	7.64	0.00
S0724	10.11	727.17
S0725	8.03	0.00
S0727	9.76	762.90
S0729	7.49	0.00
S0730	7.57	873.16
S0733	5.47	563.87
S0735	2.43	335.56

439 Thirdly, equation (3) for calculating the steady state NO concentration uses NO photoproduction
440 rates *without adjustment to ambient conditions!* This will have caused significant bias due to
441 regional and diurnal changes in sea surface irradiance and requires revision.

442 The local sea surface irradiance flux (0-873 W m⁻²) from ECMWF reanalysis data sets were used,
443 and we assumed that nitrite photoproduction rates into NO was proportional to the irradiance flux
444 (Zafiriou and McFarland, 1981), which means the rates could be adjusted to the ambient condition
445 through the solar simulator irradiance flux we have got. The average photoproduction rates of our
446 sample under local conditions were about 0.5×10⁻¹² mol L⁻¹ s⁻¹. Besides, the pH and temperature
447 influence were ignored (firstly, the linear relationship between temperature with rates was not
448 significant; secondly, for lower nitrite concentration, the photoproduction rates seemed not so
449 influenced by temperature from 20 °C to 30 °C)

450 “Since the measured [NO] were not available from the cruise, we estimated [NO] by assuming that
451 (1) NO production is mainly resulting from NO₂⁻ photodegradation and (2) the NO photoproduction
452 R_{NO} as measured in our irradiation experiment is balanced by the NO scavenging rate R_s (3) rates
453 of nitrite photoproduction into NO was proportional to the irradiance flux in order to adjust the rates
454 under simulator light into ambient light at the sampling time (Zafiriou and McFarland, 1981;
455 Olasehinde et al., 2010):

$$456 R_{NO} \times \frac{I_{ambient}}{I_{simulator}} = [NO] \times R_s, \quad (EQ 11)$$

457 where R_s represents the sum of the rate constants for the scavenging compounds reacting with NO
458 times the concentrations of the scavenger compounds.”

459 The authors also don't discuss uncertainty in the scavenging rate. Their calculations are based on
460 Olasehinde et al. (2010) who conducted their work with seawater collected from the Seto Inland
461 Sea. Is it plausible to assume that scavenging rates in the Seto Inland Sea and the tropical Pacific
462 are comparable? Please discuss this issue.

463 The uncertainty in the scavenging rate of and the lifetime of NO in seawater was discussed as below:

464 “In the study of Zafiriou et al. (1980) and Anifowose and Sakugawa (2017), they reviewed the NO
465 lifetime in the different area for the Kurose River (0.05–1.3 s), the Seto Inland sea (1.8–20 s), and

466 the central Equatorial Pacific (40-200 s, 170 E Equatorial regions), which showed an increasing
467 trend from river to open sea. It seemed that NO lifetime in our study area should be most similar to
468 the central Equatorial Pacific. Considering part of our sampling stations were in open sea while
469 some stations were closer to continent like New Guinea Island and Japan, we think that average
470 lifetime about 100 s, however the uncertainty was not reported in the literature, but estimated
471 uncertainty about 30% might be appropriate.”

472 And, finally, this section requires quantitative comparisons to previous work (=> NO concentration?,
473 flux densities?). See also my above **General Comments** on this issue.

474 **Table 1 summarized NO concentrations and NO flux densities. Besides, we also add quantitative**
475 **comparisons to previous work in revised manuscript as follows:**

476 “[NO] was estimated to range from 0 to 292×10^{-12} mol L⁻¹ (0 means that sampling time during
477 nighttime), with an average of 49×10^{-12} mol L⁻¹, which was consistent with previous results in the
478 central equatorial Pacific (46×10^{-12} mol L⁻¹), while it was lower than near continent seawater like
479 the Seto Inland Sea (up to 120×10^{-12} mol L⁻¹) and the Jiaozhou Bay (157×10^{-12} mol L⁻¹), which
480 might be because of higher nitrite concentration. NO showed lowest concentration in the Kurose
481 River, which might because of less nitrite, and shortest life time might also accounted for this in
482 river water than seawater (Anifowose and Sakugawa, 2017).

483 The resulting flux density of NO for WTNP ranged from 0 to 13.9×10^{-12} mol m⁻² s⁻¹, with an
484 average of 1.8×10^{-12} mol m⁻² s⁻¹, which is in good agreement with that in the central equatorial
485 Pacific (see Table 1), while it was lower than that in costal seawater such as the Seto Inland Sea or
486 the Jiaozhou Bay, consistent with NO concentration distribution.”

487 **Lines 253 ff, Depth integrated photoproduction:** In the absence of apparent quantum yield the
488 broadband approach taken here may be legitimate. However, there are various issues with the data
489 used:

490 Firstly, it is unclear if the irradiance data used reflect the conditions in the study area. Ideally, the
491 authors should use global irradiance levels recorded during their transects, but again-if this was not
492 possible-ECMWF ERA-5 data could be used. Solar simulator intensity is given as 725 W m^{-2} , which
493 contradicts the statement in Methods (765 W m^{-2}).

494 The solar simulator intensity 725 W m^{-2} was corrected to 765 W m^{-2} . As mentioned above, we got
495 the ECMWF ERA-5 hourly.

496 “ I_{ocean} was set to 185 W m^{-2} , while I_{ss} was 765 W m^{-2} in our study”

497 Secondly, KD could have been estimated from CDOM absorbance, but no observations were
498 reported (apart from the vague statement in Line 211). However, in the absence of CDOM or
499 attenuation data, the authors could have used recent models such as that of Smyth (2011). The 10%
500 residual light level depths given in Smyth (2011) suggest KD (365) values near 0.05 m^{-1} for the
501 study area, two times lower than the assumed value of 0.1 m^{-1} .

502 The CDOM absorbance was measured according to the method mentioned above, we tried to search
503 the calculation using CDOM to estimate the Kd (354), and we found that Kd was derived from the
504 slope of log-transformed $E_d(z, \lambda)$ versus depth (Kieber et al., 2009) In Uher (1996), where $K_d =$
505 $\frac{4}{3}(a + a_w)$, a is the light absorption coefficient of CDOM and $a_w = 0.0463 \text{ m}^{-1}$ is the light
506 absorption coefficient of pure seawater at 350 nm. However in this way, average Kd was about 0.24
507 m^{-1} , which was higher than the expected value. Besides, we tried to find other methods to estimate
508 the Kd value but failed. So the value of 0.05 m^{-1} (354 nm) in the suggested literature of Smyth,
509 (2011) was adopted.

510 “In Smyth (2011), K_{D-340} to K_{D-380} derived from 10% residual light level depths ranged from 0.04
511 m^{-1} to 0.07 m^{-1} for our study area (Smyth, 2011), we used the average value of 0.05 .”

512 Thirdly, the text in this section only gives the range of observed MLDs and does not clarify what
513 MLD value was used in the calculations.

514 MLD is the estimated mixed layer depth at the sampling station. The MLD was taken as the layer
515 depth where the temperature was $0.2 \text{ }^\circ\text{C}$ lower than the 10 m near-face seawater layer (Mont égut,
516 2004), ranging from 13–77 m with an average of 37 m. Actually, we calculated R_{ocean} respectively
517 and then we get an average value of R_{ocean} and we don't use the average MLD value in the
518 calculations.

519 “The MLD was taken as the layer depth where the temperature was 0.2°C lower than the 10 m near-
520 face seawater layer (Mont égut, 2004), ranging from 13–77 m with an average of 37 m.”

521 And, finally, it is unclear why 365 nm was used. The choice of 365 nm here contradicts the earlier
522 statement on spectral nitrite absorbance (lines 187 ff). Chu and Anastasio (2007) (wrongly cited
523 here as Liang and Cort 2007) suggest maximum nitrite photolysis closer to 340 nm although depth
524 integration likely will lead to a red shift. This requires clarification.

525 The 365 value was corrected to 354 as Chu and Anastasio (2007) and Zuo and Deng (1998). It was
526 an error that we used the value of 356 nm (the most maximum absorption wavelength of nitrite) as
527 the chosen wavelength value of the K-d, but we wrote it wrong as 365 nm.

528 About spectral nitrite absorbance experiment, we found that the rates under full-
529 band>UVA>UVB>visible, which was not consistent with single wavelength characteristic in the
530 study by Chu and Anastasio (2007), under single wavelength light, quantum yield of OH decreased
531 with the wavelength (Figure 2: 280 nm to 360 and plateau until 390) which meant that single
532 wavelength light of UVB had higher photoproduction rate than UVA. Since it might be because of
533 the wide band of UVA (320–420 nm) that lead to the total higher rates under UVA than UVB (in our
534 system 300-320).

535 “As described above, UVA is the most influencing wavelength and it is reported that 354 nm is
536 primarily responsible for NO production (Chu and Anastasio, 2007; Li et al., 2011; Zafiriou and
537 McFarland, 1981)”

538 **Editorial:** The wording could be improved by careful editing.

539 We would carefully modify our manuscript and make it improved.

540 The following references were added.

541 Babin, M., Stramski, D., Ferrari, G. M., Claustre, H., Bricaud, A., Obolensky, G., and Hoepffner, N.:
542 Variations in the light absorption coefficients of phytoplankton, nonalgal particles, and dissolved
543 organic matter in coastal waters around Europe, *J Geophys Res-Oceans*, 108(C7), 3211, 2003.

544 Blough, N. V., Zafiriou, O. C., and Bonilla, J.: Optical absorption spectra of waters from the Orinoco
545 River outflow: Terrestrial input of colored organic matter to the Caribbean, *J Geophys Res-Oceans*,
546 98, 1993.

547 Carpenter, L. J., and Nightingale, P. D.: Chemistry and Release of Gases from the Surface Ocean, *Chem.*
548 *Rev.*, 115, 4015-4034, 2015.

549 Kieber, J. D., Toole, A., Dierdre., and Kiene, P., Ronald.: Chromophoric Dissolved Organic Matter
550 Cycling during a Ross Sea Phaeocystis antarctica Bloom, in: *Smithsonian at the poles : contributions*
551 *to International Polar Year science*, edited by: Igor Krupnik, A.Lang, M., and Miller, S. E., 4,
552 *Smithsonian Institution Scholarly Press, Washington, D.C.*, 380, 2009.

553 Li, Y., Mao, Y., Liu, G., Tachiev, G., Roelant, D., Feng, X., and Cai, Y.: Degradation of methylmercury
554 and its effects on mercury distribution and cycling in the Florida Everglades, *Environ. Sci. Technol.*,
555 44, 6661-6666, 2010.

556 Loh, A. N., Bauer, J. E., and Druffel, E. R.: Variable ageing and storage of dissolved organic components
557 in the open ocean, *Nature*, 430, 877-881, 2004.

558 Minero, C., Chiron, S., Falletti, G., Maurino, V., Pelizzetti, E., Ajassa, R., Carlotti, M. E., and Vione, D.:
559 Photochemical processes involving nitrite in surface water samples, *Aquat. Sci.*, 69, 71-85, 2007.

560 Mopper, K., and Zhou, X.: Hydroxyl radical photoproduction in the sea and its potential impact on marine
561 processes, *Science*, 250, 661-664, 1990.

562 Smyth, T. J.: Penetration of UV irradiance into the global ocean, *J Geophys Res-Oceans*, 116, C11, 2011.

563 Tugaoen, H. O. N., Herckes, P., Hristovski, K., and Westerhoff, P.: Influence of ultraviolet wavelengths
564 on kinetics and selectivity for N-gases during TiO₂ photocatalytic reduction of nitrate, *Appl Catal*
565 *B-environ*, 220, 597-606, 2018.

566 Wanninkhof, R.: Relationship between wind speed and gas exchange over the ocean revisited, *Limnol.*
567 *Oceanogr.: Methods*, 12, 351-362, 2014.

568 Warneck, P., and Williams, J.: *The Atmospheric Chemist's Companion*, Springer Netherlands, 2012.

569 Weiss, R. F., and Price, B. A.: Nitrous oxide solubility in water and seawater, *Mar. Chem.*, 8, 347-359,
570 1980.

571 Zellner, R., Exner, M., and Herrmann, H.: Absolute OH quantum yields in the laser photolysis of nitrate,
572 nitrite and dissolved H₂O₂ at 308 and 351 nm in the temperature range 278–353 K, *J Atmos Chem*,
573 10, 411-425, 1990.

574 Zhu, W. Z., Zhang, J., and Yang, G. P.: Mixing behavior and photobleaching of chromophoric dissolved
575 organic matter in the Changjiang River estuary and the adjacent East China Sea, *Estuarine, Coastal*
576 *Shelf Sci.*, 207, 422-434, 2018.